Synthesis, Characterization, and Biodegradation of Maleic Anhydride, Ethylene Glycol-Copolymerization Modified Poly(D,L-Lactide Acid) and Their Crosslinked Products

Meina Huang,[1,2] Yuanliang Wang,[1,2] Yanfeng Luo[1,2]

[1]*Key Laboratory of Biorheological Science and Technology, Bioengineering College, Chongqing University, Ministry of Education, China*
[2]*National 985 Research Center of Bioinspired Material Science and Engineering, Bioengineering College, Chongqing University, Ministry of Education, China*

Received 22 December 2009; accepted 25 April 2010
DOI 10.1002/app.32692
Published online 14 July 2010 in Wiley InterScience (www.interscience.wiley.com).

ABSTRACT: Novel maleic anhydride (MAH), ethylene glycol oligomer-modified poly(D,L-lactide acid) (PEMLA), and crosslinked-PEMLA were synthesized via a series of chemical bulk modification. Briefly, MAH copolymerized with ethylene oligomer [EGO (including EG, PEG200, PEG400)] to give the PEMA; thereafter, D,L-lactide (DLLA) and prepolymers (PEMA) copolymerized to produce the PEMLA; at last, the crosslinked-PEMLA was synthesized by free radical reaction of the PEMLA. The characterization of PEMLA and crosslinked-PEMLA showed that the introduction of hydrophilic group —O— and —CH=CH— increased the flexibility and hydrophilicity of PDLLA. Moreover, the degradation of PEMLA and crosslinked-PEMLA were determined by molar weight changes and weight loss rate, and a special method, analysis of degradation positions via ^{1}H-NMR, which indicated that the PEMLA and crosslinked-PEMLA have nice degradation, and the change of content of MAH, EGO can regulate the degradation rate of PDLLA. © 2010 Wiley Periodicals, Inc. J Appl Polym Sci 118: 3460–3470, 2010

Key words: poly(D,L-lactide acid); maleic anhydride; ethylene glycol oligomer; drug delivery carrier; bone morphogenetic protein; crosslinked polymers

INTRODUCTION

Poly(lactic acid) (PLA) is a well-known FDA-approved biodegradable material.[1,2] It has been widely used as surgical sutures, scaffolds, and drug delivery carriers for drug-controlled release.[1–5] However, when it was used as a drug delivery carrier for bone morphogenetic protein (BMP), poly(lactic acid) (PLA) has such disadvantages as high brittleness and low release rate due to its strong hydrophobicity and thus slow degradation rate the weak hydrophilicity.[4–7] To overcome these problems, many research groups focused on the chemical modifications of PLA. Common approaches involved in introducing various kinds of reactive groups by copolymerization of lactide with chemicals containing functional groups in its side chain (e.g., amino group,[8] carboxyl group,[9,10] or hydroxyl group[11]). Our group has previously grafted maleic anhydride (MAH) onto poly(D,L-lactic acid) (PDLLA) backbone via melt free radical copolymerization, by which highly reactive anhydride groups were incorporated to give MAH-grafted PDLLA (MPLA).[6,7] Then our group used a new method to graft PLA with PEG, and prepared the nanoparticles for hydrophilic drug delivery.[12,13] All above chemical modifications are featured by the introduction of some functional groups on the side chain of PLA.[6–11]

Another important approach is coupling chemicals such as poly(ethylene glycol) and its derivatives,[14,15] or acrylate[16,17] with the end groups of PLA or the backbone of the PLA.[18] The acrylate can couple with the end groups of PLA,[17] moreover, the coupled C—C double bonds were subsequently cross-linked, producing network with pendant functional groups. This is good for formation of hydrogel and applications in drug-controlled release. Compared with acrylate, MAH, which contains C—C double bond too, attracted more interests due to its better biocompatibility, highly reactive anhydride group and unique surface erosion characteristics.[19] Saito et al.[20,21] synthesized the PLA-PEG-PLA, exhibited improved flexibility compared to PLA because of the introduction of ether bonds into PLA backbone. However, the degradation rate of PLA-PEG-PLA was still

Correspondence to: M. Huang (meinahuang1982@163.com).

Contract grant sponsor: Natural Science Foundation of China; contract grant number: 30470474.
Contract grant sponsor: Natural Science Foundation of Chongqing; contract grant number: CSTC 2008AB0027.

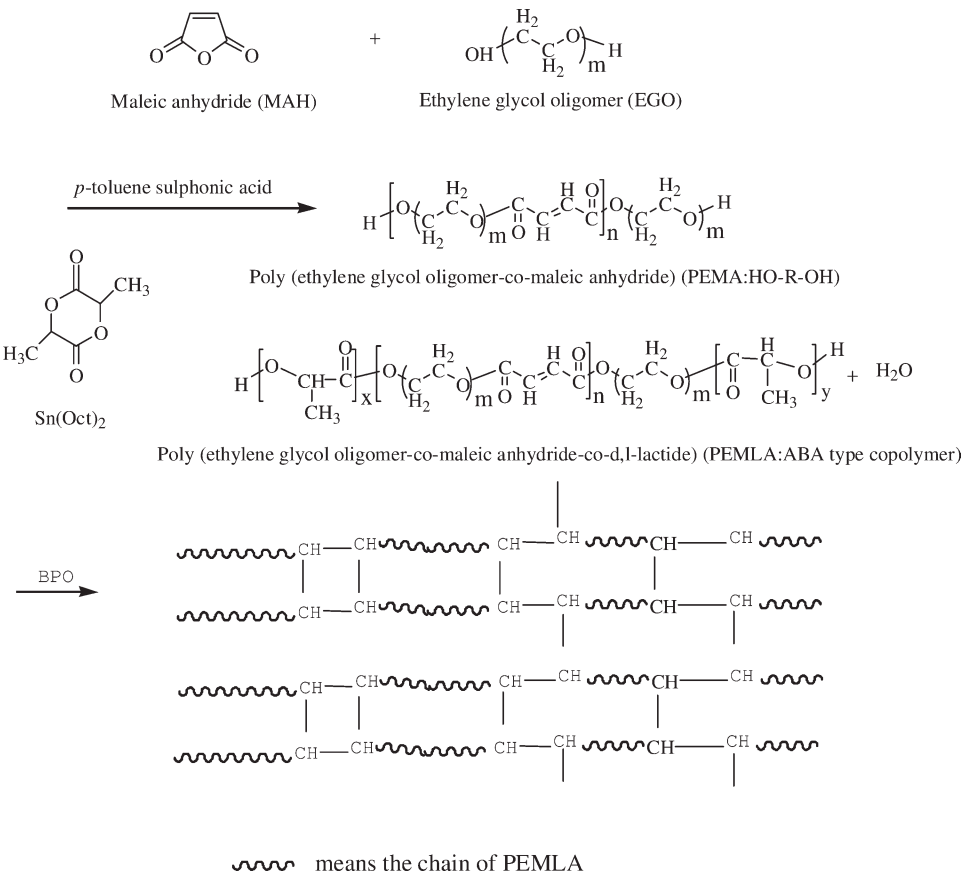

Scheme 1 Synthesis of the PEMA, PEMLA, and crosslinked-PEMLA.

somewhat slow for BMP release. Thereafter, Saito et al.[22] synthesized the poly-D,L-lactic acid-*p*-dioxanone-polyethylene glycol block copolymer. Based on previous information, the combination of hydrophilic MAH and PEG together with PLA with copolymerization reaction will hopefully create copolymers as BMP carriers that possess all advantages including improved flexibility, speeded and tunable hydrophilicity and degradation rate and thus BMP release rate.

In this study, MAH and ethylene glycol oligomer (EGO) were employed to modify the PDLLA, assuming that increasing the hydrophilic and flexible groups to PDLLA could assign good hydrophilicity, flexibility, controllable degradation, and introducing reactive groups for crosslinked reaction. The biodegradable PEMLA and crosslinked-PEMLA are potential for hydrophilic BMP delivery.

EXPERIMENTAL

Materials

D,L-lactide (DLLA) was prepared from D,L-lactic acid and purified through recrystallization with ethyl acetate in our laboratory, with a purity of greater than 99.9% (determined on model TP2080 gas chromatograph using TP-5 capillary column and hydrogen flame ionization detector. Carrier gas: N_2, flow rate: 30 mL/min). MAH, benzoyl peroxide (BPO) (Chongqing Oriental Chemical Factory) were dried at room temperature in vacuum before used. Toluene (Chongqing Oriental Chemical Factory) was treated with calcium hydride, and distilled under reduced pressure at 70°C. Ethylene glycol oligomer (EGO) containing ethylene glycol (EG), poly(ethylene glycol) (PEG) 200 or 400 ($\overline{M}_n$ = 200 or 400), *p*-toluene sulphonic acid (Chongqing Oriental Chemical Factory) were used as received. Tin(II)-2-ethylhexanoate ($Sn(Oct)_2$) was purchased from Sigma-Aldrich.

Preparation of prepolymer PEMA based on MAH and EGO

Prepolymer, poly(ethylene glycol oligomer-*co*-maleic anhydride) (PEMA) was synthesized by ring-opening polymerization of MAH with *p*-toluene sulphonic acid (Scheme 1). Predetermined amounts of MAH, EGO, *p*-toluene sulphonic acid, and toluene were added into a 250 mL three-neck round-bottomed flask, equipped with a thermometer, a magnetic stirrer and a drying tube. In addition, a purge flow of dry nitrogen was continuously introduced into the flask. Molar feed ratios of MAH to EGO

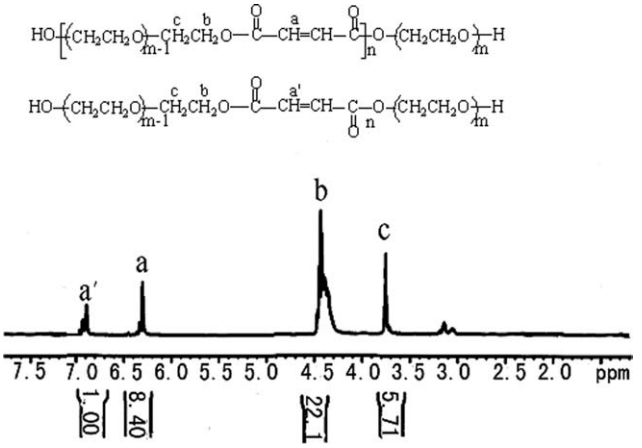

Figure 1 H-NMR of PEMA M1/EG1.2.

were 1/1.05, 1/1.2, 1/2, and *p*-toluene sulphonic acid was added by 0.12 mol % of molar amount of MAH and EGO. The mixture was heated and kept at 120°C for 24 h to give a viscous polymer. Ether was added to dissolve the unreacted MAH and then filtered the products to yield crude PEMA. The crude PEMA was rinsed thrice with ether and vacuum dried at room temperature to constant weight to give the purified prepolymer. The purified PEMA was used in following reactions, and for convenience, when the molar ratios of MAH to EGO were *x/y*, the obtained PEMA were recorded as PEMA Mx/EGy or PEMA Mx/PEG200y, PEMA Mx/PEG400y.

Preparation of ABA-type copolymers PEMLA based on DLLA and PEMA

Different weight ratios of PEMA M1/EG1.2 to DLLA (1/10, 1/5, 1/3, 1/2, 1/1) were mixed evenly in dichloromethane, and then 1/7000 $Sn(Oct)_2$ on a DLLA molar basis was added. The mixtures were vacuum dried at room temperature and then reacted at 145–150°C for 24 h. The obtained crude products were purified through coprecipitation in chloroform-alcohol system. Purified polymers were then vacuum dried at room temperature for 48 h to give the highly viscous brown ABA-type copolymer PEMLA. To simply, when the weight ratio of PEMA to DLLA was *x/y*, the obtained PEMLA was recorded as PEMLA P*x*/D*y*.

Crosslinking of PEMLA

PEMLA, 3 wt % of BPO were added into a 100 mL three-neck flask with a mechanical stirrer and a drying tube, and then DMF was added into flask. The reaction was allowed to last for 8–12 h under the nitrogen atmosphere at 80–110°C. After the reaction, the solution was dropped into excessive deionized water, the filtered fibrous solid was precipitated thrice and then dried at room temperature to constant weight to yield the desired crosslinked-PEMLA.

Characterization

Nuclear magnetic resonance (NMR) spectra were recorded at 500 MHz on a Bruker AV-500 nuclear magnetic resonance spectrometer with Bruker software using $CDCl_3$ (Fluka chemica, deuteration degree not less than 99.8%) as a solvent. Monomer compositions and number-average molecular weight ($\overline{M}_n$(NMR)) of obtained polymers were calculated from peaks area of ^{1}H NMR spectra. The characteristic peaks include I_a, $I_{a'}$ (Fig. 1) from unsaturated group of MAH, and I_c (Fig. 1) from —CH_2— of EG or PEG200/PEG400.

Molecular weights of PEMA and PEMLA were also determined by other methods. Based on molar feed ratios of EGO [including EG, PEG200 ($\overline{M}_n$ = 200) and PEG 400 ($\overline{M}_n$ = 400)] to MAH and PEMA to DLLA, $\overline{M}_n$(Theo) of PEMA and PEMLA were calculated with the eqs. (1) and (2), respectively.

$$\overline{M}_n(\text{Theo})(\text{PEMA}) = 98\frac{1}{n-1} + \overline{M}_n(\text{EGO})\left(\frac{1}{n-1} + 1\right) - 18\frac{1}{n-1} \quad (1)$$

$$\overline{M}_n(\text{Theo})(\text{PEMLA}) = \overline{M}_n(\text{Theo})(\text{PEMA}) + 144\text{m} \quad (2)$$

where n means the ratio of EGO to MAH, and m is the molar ratio of DLLA to PEMA, 98 and 18 are the $\overline{M}_n$ of MAH and H_2O (the by-product in the progress of synthesis of PEM A), 144 is the $\overline{M}_n$ of DLLA. equation (1) is established, according to the theoretical hypothesis: MAH and EGO reacted completely, and formed the ABA-type block copolymer. equation (2) is established, according to catalytic mechanism of $Sn(Oct)_2$, EG.[23] $\overline{M}_n$(Titr) is determined with hydroxyl value trimetric method. Number-average molecular weights ($\overline{M}_n$), weight-average molecular weights ($\overline{M}_w$), and polydisperity (PD) were determined from gel permeation chromatography with multiangle laser light scattering (GPC-MALLS) (laser photometer Dawn EOSTM, Wyatt Technology Corporation. The *dn/dc* value is the 0.065. The ASTRA5.1.5.0 (Wyatt technology coporation, America) and SPSS were used to calculate above parameters.). Three Agilent 1100 HPLC columns (300 × 8.0 mm) were used in series with THF as the eluent at a flow rate of 1 mL/min.

The conversion of MAH was determined on Model TP2080 gas chromatograph using TP-5 capillary column and hydrogen flame ionization detector.

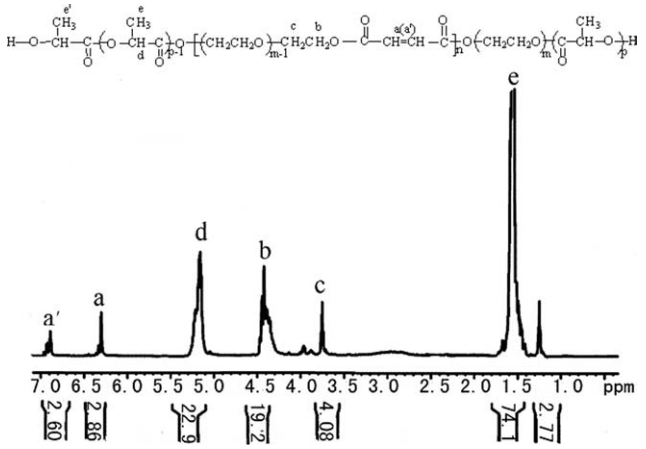

Figure 2 ^{1}H-NMR of PEMLA-1.

Carrier gas: N2; flow rate: 30 mL/min; solvent: $CHCl_3$.

Glass transition temperature (T_g) was determined by NETZSCH STA 449C differential scanning calorimetry (DSC) in a 50 mL/min flow of N_2 at a heating rate of 20°C/min ranging from −50 to 300°C.

Study of hydrophilicity of PEMLA and crosslinked-PEMLA

The hydrophilicity of PEMLA and crosslinked-PEMLA were characterized by static water contact angle and water absorption rate. For static water contact angle measurement, the polymer samples were of a dimension of 50 mm × 15 mm × 1 mm (length × width × thickness). A water-drop contact angle goniometer (Taiwan Company, Contract NO: 06IMO80) was employed to measure the static water contact angles at 25°C with a water drop of 5 μL, and the tangent leaning method was used to calculate the contact angles for all measurements.

For water absorption rate measurement, films were prepared as following method: solutions of PEMLA and crosslinked-PEMLA in $CHCl_3$ were added into glass vials (2.0 cm in diameter, 3.0 cm in height) with lids (100 mg/vial). The solution was allowed to evaporate for 72 h, and then dried in vacuum for 12 h to form film. Then the obtained circular films (2.0 cm in diameter and 250 ± 10 μm in thickness) were UV sterilized for 30 min before use for water absorption rate test. All experiments were performed at room temperature. Finally, 4 mL sterile distilled water was added to the glass vials containing films. All the vials were lidded and kept in a shaking incubator of 37 ± 0.5°C (50 strokes per min). The water absorption rate was calculated from eq. (3):

$$\text{Water absorption rate}\% = \frac{W_2 - W_1}{W_1} \times 100\% \quad (3)$$

where W_2 and W_1 are weights of the sample before and after the water absorption, respectively.

Biodegradation of PEMLA and crosslinked-PEMLA

Weight loss ratio change and molar weight change

In the study of biodegradation of polymers, sterile PBS solution (0.1 *M*, pH 7.4) was used as a medium, and 24 samples were prepared for each polymer. The preparation method of is same with that samples for water absorption rate measurement in "Study of hydrophilicity of PEMLA and crosslinked-PEMLA" section. PBS solution (4 mL) was added to the glass vials containing films. All the vials were lidded and kept in a shaking incubator of 37°C ± 0.5°C (50 strokes per min). The PBS solution was refreshed every week in the whole 8 weeks. Three vials of each polymer were taken out every week to discharge the PBS solution, and then were rinsed with distilled water and dried to constant weight in vacuum for weight loss rate measurement. The weight loss rate was calculated according to eq. (4):

$$\text{Water loss rate}\% = \frac{W_0 - W_t}{W_0} \times 100\% \quad (4)$$

where W_0 and W_t are weights of the sample before and after hydrolytic degradation, respectively.

The reported weight loss was the average of the three samples.

The molar weight of PEMLA and crosslinked-PEMLA at different degradation time were determined by Gel permeation chromatography with multiangle laser light scattering (laser photometer Dawn EOSTM, Wyatt Technology Corporation) (GPC-MALLS). The conditions are same with the measure of $\overline{M}_w$ in "Characterization" section.

Analysis of degradation positions

To investigate the degradation mechanism of PEMLA more clearly, the degradation positions of PEMLA were determined precisely by comparing the characteristic peaks area of PEMLA and its degradation products in ^{1}H-NMR spectra (Fig. 2). The characteristic peaks include the *a* and *a*′ (Fig. 2) from maleate units and fumarate units (recorded I_a and $I_{a'}$), *e* and *e*′ from methyl proton within the chain segment of DLLA units (I_e), and methyl proton in the end of the chain segment of DLLA units ($I_{e'}$), c and b from methylene adjacent to —O—C(=O)— and adjacent to —O— of EGO (including EG, PEG200, PEG400) units (I_c and I_b). During degradation, the characteristic peaks value would change, so comparing the change of peaks value can determined the degradation positions of PEMLA. Considering the reaction materials and hydrolysis of chemical bonds,

TABLE I
C—C Double Bond Contents and Molecular Weights of PEMA

Samples	$N_{un/EG}$[a] and ($N_{un/}$ EGO) (mol/mol)	$N_{un/EG}$[b] and ($N_{un/}$ EGO) (mol/mol)	$\overline{M}_n$[c]	$\overline{M}_n$ (Theo)[d]	Conversion of MAH (%)	Physical state
PEMA M1/EG1.05	0.6	0.8	1216	2900	78	Semisolid
PEMA M1/EG1.2	0.7	0.83	1050	772	86	Semisolid
PEMA M 1/EG2	0.4	0.5	772	204	84	Viscous, liquid
PEMA M1/PEG4001.2	0.8	0.83	1021	1456	91	Viscous, semisolid
PEMA M1/PEG4002	0.5	0.5	940	880	88	Viscous, liquid
PEMA M1/PEG2002	0.5	0.5	912	480	90	Viscous, liquid

[a] Calculated by I_a, $I_{a'}$, and I_c.
[b] Calculated by the molar feed ratio of MAH to EGO.
[c] Measured by the hydroxyl value from methanol solution of NaOH (NaOH/methanol) titration.
[d] Calculated by the molar feed ratio of MAH to EGO.

we determined the possible degradation positions of PEMLA (Fig. 7). To simply the calculation, $(I_a + I_{a'})/(I_e + I_{e'})$, $I_c/(I_e + I_{e'})$, $I_b/(I_e + I_{e'})$, and I_a/I_c were chose.

RESULTS AND DISCUSSION

Synthesis of prepolymers PEMA

In the study, the molar feed ratios of MAH to EGO [including EG, PEG200 ($\overline{M}_n = 200$) and PEG 400 ($\overline{M}_n = 400$)] (MAH/EGO) were 1/1.05, 1/1.2, and 1/2, and the obtained prepolymers were characterized with ^{1}H-NMR. Figure 1 is the ^{1}H-NMR spectrum of PEMA M1/EG1.2, which means that the molar feed of MAH and EG in the PEMA was 1 and 1.2. The signals at 6.4 ppm (a) and 6.9 ppm (a') were assigned to the methine of maleate units and fumarate units yielded by isomerization of maleate units, respectively, which is in agreement with the results from Nazumi et al.[3] The different structure of PEMA with maleate units and fumarate units was shown in Figure 1. The peaks at 4.2 ppm (b) and 3.8 ppm (c) were attributed to the methylene adjacent to —O— and adjacent to —O—C(=O) — of EG units, respectively.[24]

Based on I_a, $I_{a'}$ and I_c (Fig. 1), the unsaturated group content per EG unit in PEMA, which is recorded with $N_{un/EG,}$ was calculated according to eq. (5).

$$N_{un/EG} = \frac{I_a + I'_a}{I_c} \quad (5)$$

$$N_{un/EGO} = \frac{I_a + I'_a}{I_c} \quad (6)$$

In addition, $N_{un/EGO}$ (EGO include PEG200 and PEG400) was calculated by eq. (6) and listed in Table I, while the $\overline{M}_n$(Theo) and $\overline{M}_n$(Titr) were listed in Table I.

$N_{un/EG}$ or $N_{un/EGO}$ was always lower than the molar feed ratio of MAH/EG or MAH/EGO, and $\overline{M}_n$(Titr) was not conformed to the theoretical number-average molecular weight [$\overline{M}_n$(Theo)] (Table I). We can see that when the molar feed ratio of MAH to EG is 1/1.05 (Table I), $\overline{M}_n$(Titr) is lower than $\overline{M}_n$(Theo) (Table I), however, when the feeding MAH/EG are 1/1.2 and 1/2, $\overline{M}_n$(Titr) is more than $\overline{M}_n$(Theo) (Table I), and with the MAH/EG decreasing, the $\overline{M}_n$(Titr) much larger than the $\overline{M}_n$(Theo) (Table I). Moreover, the fact showed that the $\overline{M}_n$(Titr) of the PEMA from MAH and PEG200 or PEG400 (PEMA M/PEG200/PEMA M/PEG400) are much more agreement with the $\overline{M}_n$(Theo) than the PEMA from MAH and EG. These results could be attributed to two reasons. One is that when the content of MAH is high, the MAH molecule reacts with two EG molecules by condensation reaction or the ester exchange reaction. The obtained diols are less reactive than EG for further reaction with MAH, which results in the actual molecular weight decreasing and excessive MAH remaining. Alternatively, when the content of EGO (including EG, PEG200, PEG400) is high, the maleate or fumarate units attached at the end of EGO (including EG, PEG200, PEG400) partially reacted to yield EGO dimmer or trimer. From above facts, we tentatively put forward that the EG is apt to yield dimmer, trimer or oligomer and the degree of polymerization increased with the decrease of weight feed ratio of MAH to EG.

The structure of PEMA also was determined. First, the macrodiol structure can be confirmed based on the ratio of unsaturated group to EG units, which is always lower than one, and the chemical titration, including hydroxyl-value titration and carboxyl group titration, which showed the carboxyl group is near zero. Furthermore, the data in Table I and the analysis as above showed that the homo-polymerization existed in the reaction system with MAH and EG. Over the all, the structure of PEMA can be speculated, to a high extent, which is agreement with the feeding composition. The structure of PEMA M1/EG1.2 is shown in Figure 1.

TABLE II
Monomer Composition and Molecular Weights of PEMLA

	Samples	Prepolymer	Molecular weight				
			$\overline{M}_w$[a]	$\overline{M}_n$[a]	PD[a]	$\overline{M}_n$(NMR)[b]	$\overline{M}_n$(Theo)[c]
	PDLLA	–	1.78E+4	1.59E+4	1.122	–	–
PEMLA-1	PEMLA P1/D10	PEMA M1/EG1.2	1.10E+4	8.61E+3	1.274	8.53E+3	8.492E+3
PEMLA-2	PEMLA P1/D 5	PEMA M1/EG1.2	1.05E+4	7.29E+3	1.435	6.98E+3	4.63E+3
PEMLA-3	PEMLA P1/D 3	PEMA M1/EG1.2	8.91E+3	6.21E+3	1.434	6.12E+3	3.09E+3
PEMLA-4	PEMLA P1/D 2	PEMA M1/EG1.2	1.03E+4	7.45E+3	1.38	6.59E+3	2.32E+3
PEMLA-5	PEMLA P1/D 1	PEMA M1/EG1.2	2.23E+4	5.26E+3	4.251	4.32E+3	1.51E+3
PEMLA-6	PEMLA P1/D 10	PEMA M1/PEG400 1.2	2.12E+4	1.81E+4	1.174	1.68E+4	1.03E+4
PEMLA-7	PEMLA P1/D 5	PEMA M1/PEG400 1.2	2.09E+4	1.66E+4	1.261	1.43E+4	5.64E+3
PEMLA-8	PEMLA P1/D 3	PEMA M1/PEG400 1.2	2.09E+4	1.66E+4	1.261	1.43E+4	5.64E+3
	Crosslinked	PEMLA-1	4.63E+4	2.88E+4	1.6	–	–
	Crosslinked	PEMLA-2	3.60E+4	2.57E+4-	1.482	–	–
	Crosslinked	PEMLA-3	3.80E+4	2.26E+4-	1.68	–	–
	Crosslinked	PEMLA-6	5.01E+4	3.57E+4	1.4	–	–
	Crosslinked	PEMLA-7	4.2E+4	2.36E+4-	1.782	–	–
	Crosslinked	PEMLA-8	3.7E+4	2.68E+4-	1.38	–	–

[a] Determined from the MALLS-GPC.
[b] Determined from ^{1}H-NMR. $\overline{M}_n$(NMR) = 72 ($I_{1.5}/I_{1.2}$) + 98 ($I_{1.5}/3$)/$I_{(6.4+6.9)}$ + 62 ($I_{(3.8+4.2)}/4$) or $\overline{M}_n$(NMR) = 72 ($I_{1.5}/I_{1.2}$) + 98 ($I_{5.1}$)/$I_{(6.4+6.9)}$ + 62 ($I_{(3.8+4.2)}/4$).
[c] $\overline{M}_n$(Theo) represents the theoretical molecular weight calculated from the monomer feed ratio and molecular weights of repeating units.

Synthesis and characterization of PEMLA

PEMLA was synthesized by melt polymerization of DLLA and PEMA with $Sn(Oct)_2$ as an initiator at 150°C. The amount of $Sn(Oct)_2$ was 1/7000 molar ratio of DLLA. Figure 2 is the ^{1}H-NMR spectrum of PEMLA P1/D10 from PEMA M1/EG1.2, recorded PEMLA-1, which means that the molar feed of PEMA and DLLA in the copolymerization was 1/10. The signals at 5.1 ppm(d) and 1.5 ppm(e) were assigned to the methine proton and methyl proton within the chain segment of DLLA units, respectively, and the peak at 1.2 ppm (e') was assigned to the methyl proton at the end of the chain segment of DLLA units,[1] while other characteristic peaks were assigned to the protons of PEMA M1/EG1.2. The DLLA composition in PEMLA-1 $\overline{M}_n$ (NMR), $\overline{M}_n$(Theo), $\overline{M}_n$ $\overline{M}_w$ and PD from MALLS-GPC were summarized in Table II, and the detailed calculation was labeled below of Table II.

The number average molecular weight ($\overline{M}_n$) of PEMLA from MALLS-GPC were approximately agreement with the number average molecular weights determined from ^{1}H-NMR spectra [$\overline{M}_n$ (NMR)] (Table II). However, they were disagreement with the theoretical molecular weights [$\overline{M}_n$(Theo)], calculated from the weight feed ratios of PEMA to DLLA. When weight feed ratio of PEMA to DLLA increased from 1/10 to 1/1, and discrepancy increased from 1.122 to 4.251 (Table II). PEMA is used as prepolymer and coinitiator, so when the content of PEMA increase, the content of HO-R-OH is more than the necessary content of $Sn(Oct)_2$, and then the superfluous PEMA, as the chain transfer agent, can terminate the chain propagating reaction and introduce the transesterification, which may result in more than one PEMA inserting in the PEMLA chain segment, and the different $\overline{M}_w$, PD of polymers. The transesterification in the reaction can induce more activity position and the alcoholysis, thereupon the number average molecular weight ($\overline{M}_n$) of polymer decreased. Zhao et al. reported the similar regularity.[25–28]

Considering above analysis of PEMLA, the structure of PEMLA can be determined. Generally, the ring-opening polymerization of DLLA proceeded mostly as random copolymerization. However, because of the mechanism of the initiation, the

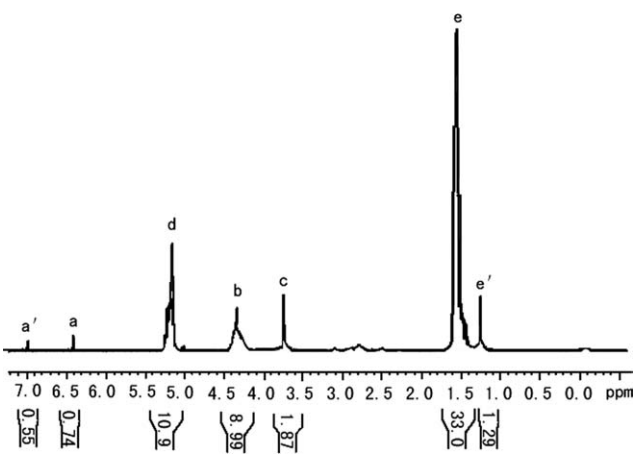

Figure 3 ^{1}H-NMR of crosslinked-PEMLA-1.

TABLE III
Glass Transition Temperature (T_g) of the PEMLA and the Crosslinked PEMLA

	Prepolymer	T_g (°C)
PEMLA-1	PEMA M1/EG 1.2	50.1
PEMLA -2	PEMA M1/EG 1.2	46.7
PEMLA -3	PEMA M1/EG 1.2	41.3
PEMLA-6	PEMA M1/PEG400 1.2	53.2
PEMLA-7	PEMA M1/PEG400 1.2	49.0
PEMLA-8	PEMA M1/PEG400 1.2	43.2
Crosslinked PEMLA-1	PEMLA-1	59.3

PEMLA most possible is block structure, and the PDLLA structure connected to the two terminals.[14,29] Since the weight feed ratio of PEMA to DLLA decreased from 1/1 to 1/10, PEMLA was expected to have increasing lactic acid repeating units on the both ends of PEMA block. The sequence of PEMLA P1/D10 (PEMLA-1 in Table II) was analyzed with ^{1}H-NMR spectrum. Considering signals at 1.2–1.5 ppm were assigned to the methyl proton, we calculate the block length, and then the average block length that 53.4 were calculated. At last, the structure of PEMLA was showed in Figure 2.

Crosslinking of PEMLA

Scheme 1 showed the crosslinked-PEMLA, the different PEMLA chain were crosslinked by free radical reaction with BPO as the initiator at 80°C for 8 h. The crosslinked specimens were white powder. The solubility of crosslinked specimens decreased. The insoluble fraction of crosslinked-PEMLA was 40 wt % after soaked in chloroform at room temperature for 1 day at standing. This may be attributed to the formation of cyclobutane. Figure 3 is the ^{1}H-NMR spectrum of the soluble fraction in deuterated chloroform of crosslinked-PEMLA-1, which showed small signal at 6.4–6.9 ppm (*e* and *e'*). The results implied that the intermolecular crosslinking had occurred on the unsaturated group.

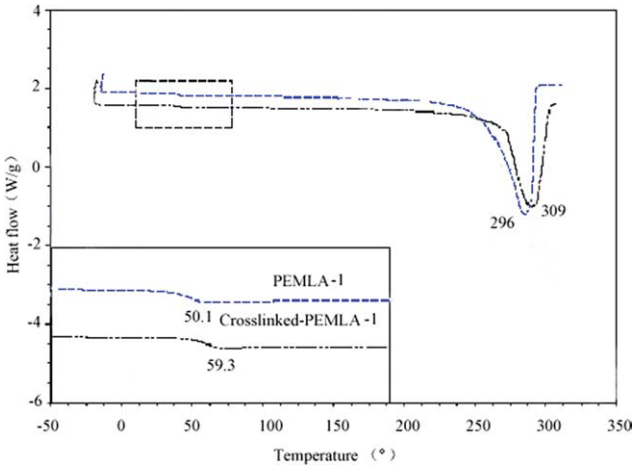

Figure 4 Thermogram of PEMLA-1 and crosslinked-PEMLA-1. [Color figure can be viewed in the online issue, which is available at www.interscience.wiley.com.]

Furthermore, the degree of crosslinking of PEMLA-1, PEMLA-2, PEMLA-3, PEMLA-6, PEMLA-7, and PEMLA-8 were determined to be 3.34, 3.52, 3.63, 1.97, 1.42, and 1.61 by eq. (7), respectively. The results showed that more unsaturated and low molecular weights are beneficial to the crosslinking reaction. Therefore, we preliminarily conjectured that the crosslinking reaction was affected by two reasons: the content of unsaturated groups, and the molecular weighs ($\overline{M}_n$) of PEMLA.

$$D = \frac{\overline{M}_{n_{-\text{crosslinked PEMLA}}}}{\overline{M}_{n_{-\text{PEMLA}}}} \quad (7)$$

TABLE IV
Static Water Contact Angle and Water Absorption Ratio of PEMLA and Crosslinked-PEMLA

	Samples	Prepolymer	Static water contact angle (°)	Water absorption (%)
	PDLLA	–	75.5	21.4 ± 0.12
PEMLA-1	PEMLA P1/D10	PEMA M1/EG1.2	74.5	24.6 ± 0.18
PEMLA-2	PEMLA P1/D 5	PEMA M1/EG1.2	71.3	30.9 ± 0.22
PEMLA-3	PEMLA P1/D 3	PEMA M1/EG1.2	70.1	29.9 ± 0.18
PEMLA-4	PEMLA P1/D 2	PEMA M1/EG1.2	69	48.8 ± 0.26
PEMLA-5	PEMLA P1/D 1	PEMA M1/EG1.2	64.5	51.1 ± 0.29
PEMLA-6	PEMLA P1/D 10	PEMA M1/PEG400 1.2	75.1	29.9 ± 0.12
PEMLA-7	PEMLA P1/D 5	PEMA M1/PEG400 1.2	73.9	28.9 ± 0.11
PEMLA-8	PEMLA P1/D 3	PEMA M1/PEG400 1.2	73.9	28.9 ± 0.11
	Crosslinked	PEMLA-1	77.2	17.8 ± 0.15
	Crosslinked	PEMLA-2	78.1	19.3 ± 0.22
	Crosslinked	PEMLA-3	79.9	21.0 ± 0.06
	Crosslinked	PEMLA-6	77.8	18.1 ± 0.11
	Crosslinked	PEMLA-7	78.9	19.0 ± 0.24
	Crosslinked	PEMLA-8	79.2	20.8 ± 0.10

The detailed parameters of the polymer are showed in Table 2.

TABLE V
Characteristic Peaks Value Ratio of ^{1}H-NMR for PEMLA During Degradation

Degradation time(d)	PEMLA	$I_a/(I_e + I_{e'})$	$I_c/(I_e + I_{e'})$	$I_b/(I_e + I_{e'})$	I_a/I_c
0	PEMLA-1	0.1196	0.4367	0.089	–
3	PEMLA-1-3	0.078	0.3071	0.149	–
21	PEMLA-1-21	0.081	0.3164	0	–
30	PEMLA-1-30	0.1186	0.4196	0	–
0	PEMLA-6	0.0073	–	0.0401	0.3654
3	PEMLA-6-3	0.0079	–	0.0433	0.3653
21	PEMLA-6-21	0.0077	–	0.0371	0.4140
30	PEMLAE-6-30	0.0090	–	0.0416	0.4309

where $\overline{M}_{n\text{-crossliniedPEMLA}}$ means the $\overline{M}_n$ of crosslinked-PEMLA, $\overline{M}_{n\text{-PEMLA}}$ means the $\overline{M}_n$ of PEMLA.

Glass transition temperature (T_g) of PEMLA and crosslinked-PEMLA

The glass transition temperature (T_g) of PEMLA and crosslinked-PEMLA was investigated by low temperature differential scanning calorimetry (DSC), and are summarized in Table III. Figure 4 showed the thermogram of PEMLA-1 and crosslinked-PEMLA, from which we can know that only one glass transition was observed in each DSC thermogram of PEMLA or crosslinked-PEMLA. When the content of DLLA and $\overline{M}_n$ of EGO (62, 200 or 400) increased, T_g increased from 37 to 50°C, lower than T_g of PDLLA (56.5°C), implying that the components in copolymer was not phase-separated and properties of PDLLA were greatly affected by the modification of PDLLA with MAH and EGO.[30] The endothermal peak corresponding to crystal melt was not found in these thermograms, indicating that they are amorphous. Furthermore, it is obvious that crosslinked-PEMLA exhibited higher T_g than their corresponding PEMLA, which conformed to the report.[30]

The hydrophilicity of PEMLA and crosslinked-PEMLA

The hydrophilicity of PEMLA and crosslinked-PEMLA were summarized in Table IV. The static water contact angle was immediately measured when the water droplet was deposited on the membrane surface, which better reflects the natural wettability of the membrane material surface. Table IV showed that the static water contact angles decrease significantly after increasing of weight ratio of PEMA/DLLA in PEMLA. The contact angle decreased from 75.5 to 64.5, when the weight ratio of PEMA M1/EG1.2/DLLA increased from 1/10 to 1/1, while the contact angle decreased from 75.1 to 73.9 at the weight ratio of PEMA M1/PEG400 1.2/DLLA increased from 1/10 to 1/3. However, we can find that the contact angle of crosslinked-PEMLA showed the reverse regular. The water absorption showed the same regular. The results indicate that the instantaneous hydrophilicity (static contact angle) and long-acting hydrophilicity (water absorption) reflected the same regular. The hydrophicity of PEMLA was significantly influenced by the hydrophic chemical group, —C=C— and ether group.[3] The ether group is easier than ester group to generate hydrogen group, which is beneficial to bond the water molecular, and increases the hydrophilicity of polymer molecular. The crucial factor of affecting the hydrophilicity of crosslinked-PEMLA was the

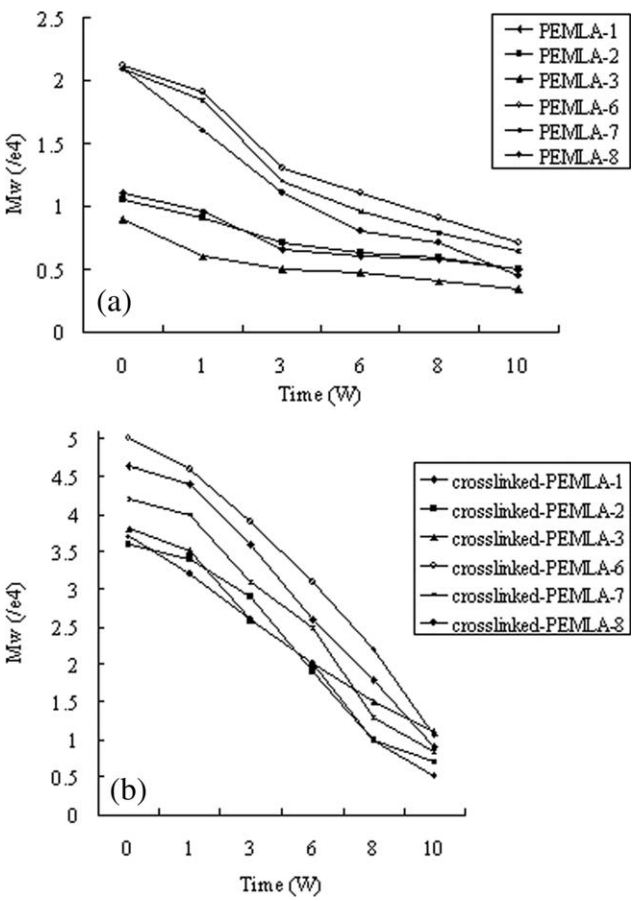

Figure 5 (a) M_w change of PEMLA with degradation time [medium: PBS (pH = 7.4, 0.2 M)] (b) M_w change of crosslinked-PEMLA with degradation time [medium: PBS (pH = 7.4, 0.2 *M*)].

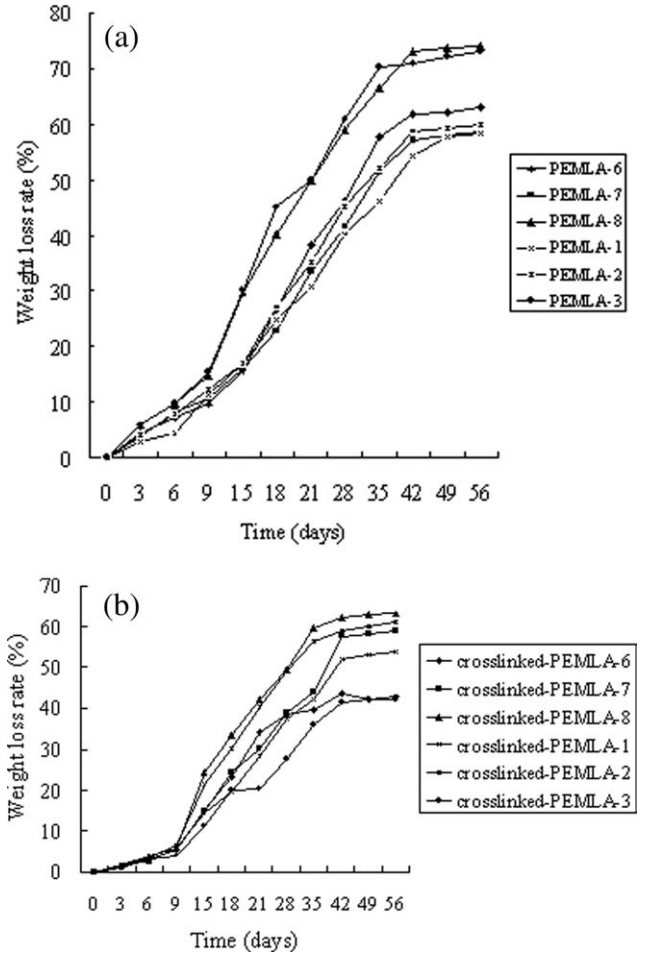

Figure 6 (a) Biodegradation test for the copolymers PEMLA. Percentage degradation was calculated from weight loss in the phosphate buffer (b) Biodegradation test for the crosslinked-PEMLA. Percentage degradation was calculated from weight loss in the phosphate buffer.

degree of crosslinking, which was affected by the content of double bond in PEMLA. The degree of crosslinking (see "Crosslinking of PEMLA section") of PEMLA-1, PEMLA-2, PEMLA-3, PEMLA-6, PEMLA-7, and PEMLA-8 were 3.34, 3.52, 3.63, 1.97, 1.42, and 1.61. The degree of crosslinking will result in the high density network structure, which may embed the hydrophilic group in the network interior, and decrease the hydrophilicity of crosslinked-PEMLA, and the degradation rate (see "The hydrophilicity of PEMLA and crosslinked-PEMLA" section) in a short time.

Biodegradation

Molar weight changes of PEMLA and crosslinked-PEMLA during degradation

The $\overline{M}_w$ of PEMLA, crosslinked-PEMLA as a function of time during a degradation in PBS solution are plotted in Figure 5. As shown in Figure 5, PEMLA and crosslinked-PEMLA with different content of double bond, network structure, respectively, hydrolyzed differently either.

The degradation of PLA is believed to occur through four consecutive steps: hydration, initial degradation, further degradation and solubilization. The similar four steps are expected for the MAH, EGO-modified-PDLLA and their crosslinked products. The first phase ends within first week for where the degradation rate is relative slow, because polymers are mainly in the hydration stage and no negligible chemical structure change. However, the degradation of PEMLA-1, 2, 3 is different with PEMLA-6, 7, 8, which can be attributed to the different hydrophilicity, so the molar weight of PEMLA-6, 7, 8 decreased by 40%.

The second phase starts from the second week for all PEMLAs. In the second phase, the changes of PEMLAs showed the downtrend. Then the degradation reached to the third, even forth stage (see "Weight loss rate change of PEMLA and crosslinked-PEMLA" section). In the initial degradation stage, the molar weights of all polymers are high and thus ester bonds could be easily and quickly cleaved. In the further degradation stage, acidity-induced auto-catalysis of all PEMLAs (with different hydrophilic chain) speed up the polymer chain cleavage. Both the high molecular weights at the initial degradation stage and the acidity-induced auto-catalysis at the further degradation stage contribute to the fast degradation rate for all PEMLAs. The obvious effects of acidity-induced auto-catalysis on molar weights of PDLLA were also observed in other PDLLA-based specimens, especially in those specimens of larger size.[31,32]

The molar weight changes of crosslinked-PEMLA were slow at initial stage of degradation. However, the molar weight changes were fast until that the molar weight reached to about 5,000 to 10,000. The slow degradation at first degradation could be attributed to the network structure, which affected the hydration stage of degradation. However, there are many hydrophilic —O— group in the crosslinked-PEMLA, so the degradation reached to the initial degradation, even further degradation.

Weight loss rate change of PEMLA and crosslinked-PEMLA

Figure 6(a,b) showed the weight loss rate of PEMLA and crosslinked-PEMLA as a function of time during incubation in PBS solution. As we can see in Figure 6(a), weight loss rate of PEMLA proceeded slowly at first 2 weeks, which is corresponding to the first degradation stage. In such stage, molecular weight of PEMLA remained too high to become solution.

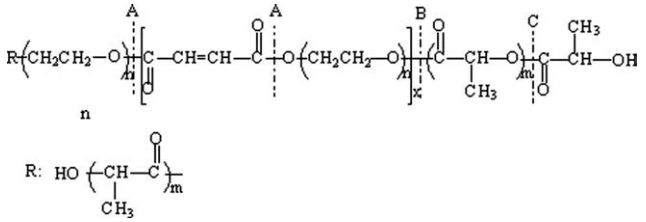

Figure 7 The degradation position of PEMLA.

Then weight loss rate increased, which mainly was attributed to that the fragments of PEMLA were further cleaved to small molecules and dissolved in aqueous incubating media. The weight loss rate of PEMLA-1, PEMLA-2, PEMLA-6, and PEMLA-7 (Table II) were 60% after degradation time of 6 weeks, while PEMLA-3 and PEMLA-8 (Table II) were more than 70%. The difference can be attributed to that PEMLA-3 and PEMLA-8 have higher hydrophilicity than PEMLA-1, PEMLA-2, PEMLA-6, PEMLA-7 (showed in Table II), because of having more PEMA, which resulted in the stronger acidity-induced autocatalysis. Furthermore, weight loss rate of PEMLA-1 ($\overline{M}_n$ = 8.61E+3, see Table II) is much more the PEMLA-6 ($\overline{M}_n$ = 1.81E+4, see Table II), which is correlated with the $\overline{M}_n$.

Figure 6(b) showed the weight loss rate of crosslinked-PEMLA. The weight loss rate of crosslinked-PEMLA was slow at the initial stage of degradation. After 10 days, the weight loss rate increased. The weight loss rate of crosslinked-PEMLA-1 ($\overline{M}_n$ = 2.88E+4, D = 4.2), PEMLA-2 ($\overline{M}_n$ = 2.57E+4, D = 3.6) were higher than crosslinked-PEMLA-3 ($\overline{M}_n$ = 2.26E+4, D = 4.4), while the weight loss rate of crosslinked-PEMLA-6 ($\overline{M}_n$ = 3.57E+4, D = 1.97) is lower than crosslinked-PEMLA-7 ($\overline{M}_n$ = 2.36E+4, D = 1.42), crosslinked-PEMLA-8 ($\overline{M}_n$ = 2.68E+4, D = 1.61). Otherwise, the weight loss rate of the crosslinked-PEMLA was lower than the corresponding PEMLA. Judging from the degradation regularity of PEMLA [see Fig. 6(a)], we preliminary put forward that the difference is attributed to following influence factors. One factor is the degree of crosslinking, which is affected by the content of unsaturated groups in PEMA. For example, we can see that the unsaturated group in PEMLA-3, PEMLA-8 are more than PEMLA-1, PEMLA-6, and the degree of crosslinking of PEMLA-3, PEMLA-8 are relative high, which is conformed to the Refs. 33 and 34. In addition, comparing the weight loss rate of crosslinked-PEMLA-1, 2, 3 to crosslinked-PEMLA-6, 7, 8 with similar $\overline{M}_n$, we can see that the weight loss rate of crosslinked-PEMLA-6, 7, 8, consist of less unsaturated group, were higher than crosslinked-PEMLA-1, 2, 3. The other factor is the different $\overline{M}_n$ of crosslinked-PEMLA. Figure 6(b) showed that the weight loss rate of crosslinked-PEMLA decreases with an increase of the $\overline{M}_n$ of PEMLA.

Considering the molar weight and weight loss rate, the weight loss rates of all polymers were much than 50–70%, however, the molar weight of crosslinked-PEMLAs were too high to dissolve in the paper after 10 weeks. It is well know that the degradation of polyester is bulk degradation, so we can presume the degradation of PEMLA and crosslinked-PEMLA was cleaved in specified positions and controllable degradation by regulating the content of hydrophilic group. The degradation position can be determined by the analysis of characteristic peaks value.

Analysis of degradation position

To deeply analyze the degradation position of PEMLA and crosslinked-PEMLA, we take the degradation of PEMLA-1 and PEMLA-6 as examples. Figure 7 shows the diagram of PEMLA-1. As one can see in Figure 7, the probable degradation positions A, B, C were pointed out based on the structure of PEMLA-1. By comparing the characteristic peak value of PEMLA-1 with its degradation products, containing PEMLA-1-3 (degradation for 3 days), PEMLA-1-21 (for 21 days), PEMLA-1-30 (for 30 days), and degradation positions were ascertainmented. To simply, the ratios of $(I_a + I_{a'})/(I_e + I_{e'})$, $I_b/(I_e + I_{e'})$, $I_c\ t/(I_e + I_{e'})$ (see "Biodegradation of PEMLA and crosslinked-PEMLA" section), in addition, $(I_a + I_{a'})/I_b$ for PEMLA-6, were chose and listed in Table V. The $(I_a + I_{a'})/(I_e + I_{e'})$, $I_b/(I_e + I_{e'})$ and $I_c/(I_e + I_{e'})$ demonstrated that the ratio of content of unsaturated group to lactic acid group, the —CH_2— [adjacent to —O— (C=O)] to lactic acid, and —CH_2— (adjacent to —O—) to lactic acid group. Otherwise, the $(I_a + I_{a'})/I_c$ meant ratio of content unsaturated group to —CH_2— (adjacent to —O—), respectively. The change regularity of these ratios can show the degradation positions indirectly.

Comparing characteristic peaks area ratios of PEMLA-1, PEMLA-1-3, PEMLA-1-21, and PEMLA-1-30, we can see the ratio of $(I_a + I_{a'})/(I_e + I_{e'})$ was on the downtrend first and then on the uptrend nd $I_b/(I_e + I_{e'})$ was on the uptrend, and then to zero; and $I_c/(I_e + I_{e'})$ was on the downtrend, and then to uptrend. At the first stage, hypothesizing the $(I_e + I_{e'})$ is constant, I_a and I_c decreased, while I_b increased, from which we can predicate the degradation occurred on position A (Fig. 7), showing the degradation occurred within the prepolymer chain segment at first. Then the $(I_a + I_{a'})/(I_e + I_{e'})$ and $I_c/(I_e + I_{e'})$ increased (see Table V), indicating that the $(I_e + I_{e'})$ start to decrease and the degradation showed up interior of PDLLA (Fig. 7). During last stage, I_b decreased to zero (see Table V), showing

the conjunction between the prepolymer and the PDLLA chain segment begin to collapse. The degradation occurred on position A and B, and resulted in the producing of ethylene alcohol, which can dissolve in the PBS easily. At the same time, comparing the degradation process of the PEMLA-6 with PEMLA-6-3, PEMLA-6-21, and PEMLA-6-30, we can see $(I_a + I_{a'})/(I_e + I_{e'})$ and $(I_a + I_{a'})/I_b$ kept constant, however, $I_b/(I_e + I_{e'})$ was on the uptrend at the beginning, manifesting that the degradation mainly occurred interior of PDLLA chain segment. After 21 days, the ratio of $(I_a + I_{a'})/I_b$ increased, $I_b/I_e + I_{e'})$ decreased and $(I_a + I_{a'})/(I_e + I_{e'})$ have little increase comparing with PEMLA-6 (Fig. 3), indicating the degradation begin to occurred between the PEMA and PDLLA and interior of PEMA. The different degradation of PEMLA-1 with PEMLA-6 may be due to the different hydrophilicity (see "The hydrophilicity of PEMLA and crosslinked-PEMLA" section).

From the structure, degradation curve of PEMLA and corresponding crosslinked-PEMLA, we presumed that the degradation position of crosslinked-PEMLA are similar with PEMLA, however, the degree of crosslinking played an important role in the degradation.

CONCLUSIONS

The PDLLA was modified by MAH, and ethylene glycol oligomer (EGO) via copolymerization reaction by a series chemical reaction. In addition, the crosslinked products of the modified-PDLLA (PEMLA) was prepared by free radical reaction. The glass transition temperature (T_g) of PDLLA decreased, with the increase of content of MAH and ethylene glycol oligomer (including EG, PEG200, PEG400). T_g is the important parameter of flexibility of polymer, so we can know that the introduction of MAH, EGO can increase the flexibility of PDLLA, and overcome the brittleness of PDLLA, which is beneficial to the application of drug release. In addition, the hydrophilicity measurement showed that the introduction of MAH, EGO with hydrophilic group ether bond and double bond increase the hydrophilicity, which promotes the degradation rate. In the study, the degradation mechanism and degradation positions of the modified-PDLLA were detailed discussed by molar weight and weight loss rate measurement and the chemical bond analysis, which is the novelty of the paper. The degradation measurement showed the degradation is controllable by changing of content of MAH, EGO in backbone of PDLLA.

References

1. Shi, P. J.; Li, Y. G.; Pan, C. Y. Eur Polym J 2004, 40, 1283.
2. Wang, S. F.; Lu, L. C.; Gruetzmacher, J. A.; Currier, B. L.; Yaszemski, M. J. Biomaterials 2006, 27, 832.
3. Teramoto, N.; Kogure, H.; Kimura, Y.; Shibata, M. Polymer 2004, 45, 7927.
4. Kim, K.; Yu, M. K.; Zong, X. H.; Chiu, J.; Fang, D. F.; Seo, Y. S.; Hsiao, B. S.; Chu, B.; Hadjiargyrou, M. Biomaterials 2003, 24, 4977.
5. Gupta, B.; Revagade, N.; Hilborn, J. Prog Polym Sci 2007, 32, 455.
6. Luo, Y. F.; Wang, Y. L.; Niu, X. F.; Pan, J.; Shi, L. P. Chin Chem Lett 2004, 15, 521.
7. Niu, X. F.; Wang, Y. L.; Luo, Y. F.; Pan, J.; Shi, L. P.; Guo, L. X. Chin Chem Lett 2004, 16, 1035.
8. Drumheller, P. D.; Hubbell, J. A. Anal Biochem 1994, 222, 380.
9. Taguchi, K.; Yano, S.; Hiratani, K.; Minoura, N.; Okahata, Y. Macromolecules 1988, 21, 3338.
10. Elisseeff, J.; Anseth, K.; Langer, R.; Hrkach, J. Macromolecules 1997, 30, 2182.
11. Arvanitoyannis, I.; Nakayama, A.; Kawasaki, N.; Yamamoto, N. Polymer 1995, 36, 2947.
12. Pan, J.; Zhao, M. M.; Liu, Y.; Wang, B.; Mi, L.; Yang, L. J Biomed Mater Res Part A 2009, 89, 160.
13. Wang, B.; Pan, J.; Liu, Y.; Mi, L.; Zhang, T. X. Acta Chim Sinica 2008, 66, 487–491. (In Chinese)
14. Korhonen, H.; Helminen, A.; Seppala, J. V. Polymer 2001, 42, 7541.
15. Otsuka, H.; Nagasaki, Y. In Proceedings of the 22nd annual EMBS International Conference, Chicago, 2000.
16. Gearaldine, G.; Lowe, C.; Pechy, P.; Kausch, H. H.; Hihorn, J. J Mater Sci Mater Med 2000, 11, 505.
17. Reddy, S. K.; Anseth, K. S.; Bowman, C. N. Polymer 2005, 46, 4212.
18. Huang, M. N.; Luo, Y. F.; Wang, Y. L.; Chen, J.; Li, Y. G.; Fu, C. H. Chin Chem Lett 2007, 18, 605.
19. Tang, J. W.; Wang, J. W.; He, Y. D.; Tong, Z. S.; Shen, Z. S.; Li, X. G.; Li, B. X. Prog Org Coat 2008, 63, 195.
20. Saito, N.; Okada, T.; Toba, S.; Miyamoto, S.; Takaoka, K. J Biomed Mater Res 1999, 47, 104.
21. Saito, N.; Okada, T.; Toba S.; Horiuchi, H.; Murakami, N.; Takahashi, J.; Nawata, M.; Ota, H.; Miyamoto, S.; Nozaki, K.; Takaoka, K. J Bone Joint Surg Am 2001, 83-A (Suppl 1, Part 2): S92.
22. Saito, N.; Murakami, N.; Takahashi, J.; Horiuchi, H.; Ota, H.; Kato, H.; Okada, T.; Nozaki, K.; Takaoka, K. Adv Drug Deliv Rev 2005, 57, 1037.
23. Baimark, Y.; Molloy, R. Sci Asia 2004, 30, 327.
24. Luo, Y. F.; Wang, Y. L.; Niu, X. F.; Fu, C. H.; Wang, S. J. Eur Polym J 2007, 43, 3856.
25. Zhao, J.; Quan, D. P.; Liao, K. R.; Wu, Q. Chem J Chin Univ Chin 2005, 26, 1570 (In Chinese).
26. Jedlinskiz, Z.; Kurcok, P.; Walach, W.; Janeozek, H.; Radecka, L. Macromol Chem 1993, 194, 1681.
27. Zhu, Z. X.; Xiong, C. D.; Zhang, L. L.; Yuan, M. L.; Deng, X. M. Eur Polym J 1997, 35, 1821.
28. Kubies, D.; Rypacek, F.; Kovarova, J.; Lednicky, F. Biomaterials 2002, 21, 529.
29. Piao, L. H.; Deng, M. X.; Chen, X. S.; Jiang, L. S.; Jing, X. B. Polymer 2003, 44, 2331.
30. Chrissafis, K.; Paraskevopoulos, K. M.; Bikiaris, D. N. Polym Degrad Stab 2006, 91, 60.
31. Pitt, C. G.; Gratzel, M. M.; Kimmel, G. L.; Surles, J.; Schindler, A. Biomaterials 1981, 2, 215.
32. Grizzi, I.; Garreau, H.; Li, S.; Vert, M. Biomaterials 1995, 16, 305.
33. Luo, B. H.; Quan, D. P.; Liao, K. R.; Lu, Z. J.; Zhou, C. R. Acta Polym Sinica 2005, 3, 327.
34. Clapper, J. D.; Skeie, J. M; Mullins, R. F.; Allan Guymon, C. Polymer 2007, 48, 6554.